

Receptivity Considerations for Cascaded Actuators Generating Tollmien-Schlichting Waves

Marcus Zengl and Ulrich Rist

Universität Stuttgart, IAG, Pfaffenwaldring 21, D-70550 Stuttgart, Germany
<http://www.iag.uni-stuttgart.de>

Summary

Different blowing and suction profiles were analyzed for flow control experiments for a generic blowing-and-suction actuator. The aim of this actuator is to dampen Tollmien-Schlichting (TS) waves by superimposing a wave in counterphase. It is essential to dampen only designated waves without introducing other unstable modes. Therefore, the receptivity of the TS waves to the introduced disturbances is an issue. Actuator cascades of multiple actuator elements were investigated for time-periodic forcing. Design parameters and their influence on the ability to generate TS waves without triggering unwanted waves were investigated. Hereby, it was assumed that the spatial velocity profile of each actuator element is uniform.

1 Introduction

1.1 Objective

Reducing drag of internal and external flows has always been an issue to improve performance and cost efficiency of vehicles. Delay or even inhibition of laminar-turbulent transition is one possibility to reduce the drag caused by skin friction in wall-bounded non-separating flows. Our objective is to reduce the amplitude of so-called Tollmien-Schlichting waves—responsible for laminar-turbulent transition—by blowing and suction at the wall. Introducing a TS wave of the same amplitude but opposite phase to the wave to be damped results in cancellation of both waves. Applying this technique in the linear regime, before secondary instability sets in, can delay transition considerably [2]. On the other hand, the generation of counterphase waves can unintentionally trigger additional TS waves, promoting the transition process. Applying a time-periodic sinusoidal input signal on a blowing-and-suction actuator does not imply that the slot velocity over time is purely sinusoidal. The output signal contains higher harmonics which are able to trigger higher harmonics of the TS wave to be generated. Our approach is to design the actuator in such a way that it can generate TS waves of multiple frequencies (respectively wavenumbers) while keeping the receptivity of the according higher harmonics as low as possible.

1.2 Previous Investigations

Depending on blowing ratio, spatial distribution, frequency, and spanwise wavenumber the laminar boundary layer reacts differently on excitations by a disturbance strip. Gmelin [1] has found a linear dependence of the effective wave amplitude of a generated TS wave on the Fourier transform of the spatial wall-normal velocity profile at the disturbance strip. Due to the generation of a mixture of modes above the disturbance strip in his direct numerical simulation, he has used a reference simulation with a generated TS wave further upstream. By comparison of both simulations at a control point some wavelengths downstream of the disturbance strip, he determined the effective amplitude of the designated TS wave at the location of the disturbance strip. For a Blasius boundary layer, Gmelin's receptivity constant, i.e. the ratio of the effective wave amplitude to the Fourier-transformed wall-velocity, decreases with increasing frequency.

2 Method

2.1 Wall-Velocity Actuation

At the actuator slot a wall-normal velocity v_w is prescribed. We assume spanwise periodicity and time-periodic blowing and suction. Please note that any non-sinusoidal time-periodic actuation with a period of $T = \frac{2\pi}{\omega}$ can be Fourier-transformed such that the wall-normal velocity can be written as

$$v_w = v_x(x) \cos(\beta z) \sum_{h=1}^{\infty} A_h \cos(h\omega t + \phi_h) . \quad (1)$$

2.2 Receptivity Considerations

For two-dimensional waves, i.e. $\beta = 0$, we apply a Fourier transform on the spatial amplitude distribution v_x with respect to the streamwise wavenumber α

$$V_x(\alpha) = \int_{-\infty}^{\infty} v_x(x) e^{-i\alpha x} dx . \quad (2)$$

Gmelin has shown that the ratio of the effective amplitude of a generated TS wave with the streamwise wavenumber α_{TS} divided by the Fourier integral $V_x(\alpha_{TS})$ is constant for a given frequency and velocity profile. For oblique-travelling waves the Fourier-transform has to be done in the direction of the wave propagation. However, we will focus on two-dimensional waves in this paper. The influences of different design parameters on oblique travelling waves will head in the same direction. Exemplarily, in Fig. 1 the value of the dimensionless receptivity constant

$$C_r = \frac{\tilde{u}_{TS}}{|V(\alpha_{TS})|} \frac{\nu}{U_{\infty}} \quad (3)$$

is plotted versus the dimensionsless frequency

$$F = \frac{\omega\nu}{U_\infty^2} \quad (4)$$

for the Blasius boundary layer. Here, \tilde{u}_{TS} is the effective amplitude of the generated TS wave defined by its maximum streamwise disturbance velocity. The plot was created using a correlation for the receptivity constant from Marx [3]. Marx fitted the coefficients of his ansatz function to data points obtained by evaluating the receptivity with direct numerical simulation.

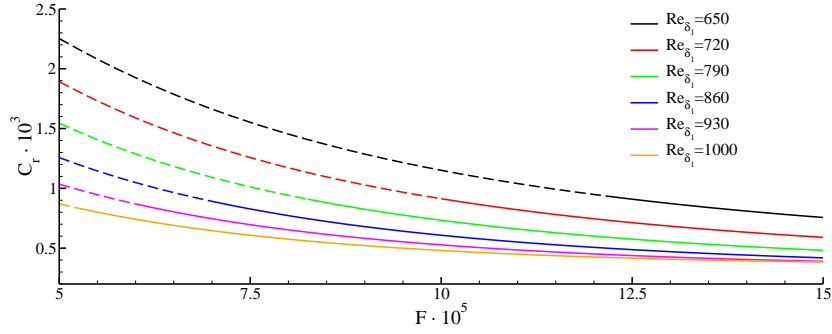


Figure 1 Receptivity constant C_r versus frequency F for different streamwise positions of the Blasius boundary layer (obtained using correlation from Marx [3]). Dashed lines denote stable waves.

2.3 Actuator Design

In order to optimize the actuator, we try to maximize $\frac{|V_x(\alpha)|}{Q}$ for the designated wavenumber α_{TS} , i.e. the wavenumber of the TS wave to be generated, and minimize it for the TS waves of its higher time harmonics. Here,

$$Q = \int_{-\infty}^{\infty} |v_x(x)| dx \quad (5)$$

is the maximum flow rate through the wall. The wavenumbers of the TS wave to be generated and its higher harmonics are given by the dispersion relation

$$D(\alpha, \beta, \omega) = 0 \quad (6)$$

where β is the spanwise wavenumber of the disturbance. Since α is monotonically increasing with increasing ω , we can say that $\frac{|V_x(\alpha)|}{Q}$ is to be minimized for wavenumbers greater than α_{TS} . The value of $|V_x(\alpha)|$ below α_{TS} has no relevance as long as we force with a period of $T = \frac{2\pi}{\omega_{\text{TS}}}$. Since in most cases the wavenumbers

of the higher harmonics with streamwise wavenumbers greater than approximately $6\alpha_{\text{TS}}$ are stable, we focus only on wavenumbers up to this value. Please note that the value of $\frac{|V_x(\alpha)|}{Q}$ can not exceed 1 and is somewhat a measure for efficiency.

In order not to lose generality, the length of the actuator cascade is further scaled to unit length. Each actuator element is then $L_e = \frac{1}{N}$ wide where N is the number of actuator elements. The uniform wall velocity $v_{x,j}$ of an element j is taken to be

$$v_{x,j} = \sin(\alpha_{\text{TS}}x_j + \theta) \quad (7)$$

to achieve a large $V_x(\alpha_{\text{TS}})$ where x_j is the coordinate of the slot center of element j . This leads to the spatial amplitude distribution

$$v_x = \begin{cases} 0 & \text{for } x < 0, \\ \sin\left(\alpha_{\text{TS}}\frac{2[Nx]-1}{2N} + \theta\right) & \text{for } 0 \leq x < 1 \wedge \left|x - \frac{2[Nx]-1}{2N}\right| \leq \frac{\Xi}{2N}, \\ 0 & \text{for } 0 \leq x < 1 \wedge \left|x - \frac{2[Nx]-1}{2N}\right| > \frac{\Xi}{2N}, \\ 0 & \text{for } 1 \leq x, \end{cases} \quad (8)$$

with the ratio of the slot width to the element width $\Xi \in (0, 1)$, a phase parameter $\theta \in [0, \frac{\pi}{2}]$, and the number of actuator elements N which are to be chosen. Consequently, a descriptive comparison of the amplitude distribution function is that of a continuous sine function $v_x = \sin(\alpha_{\text{TS}}x_j + \theta)$ for $0 \leq x < 1$, which is zero for all other values of x . A sketch of an actuator cascade with three elements is drawn in Fig. 2. The walls of the different actuator elements are shaded, and the velocity

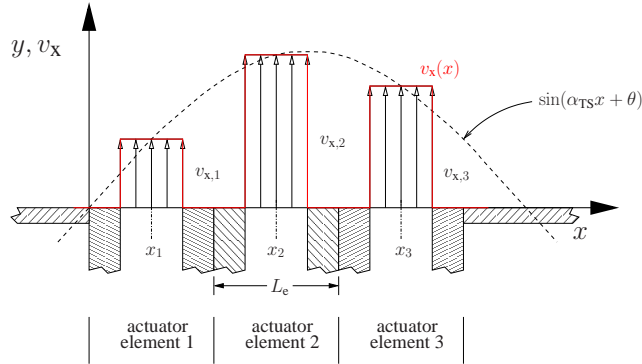


Figure 2 Sketch of three cascaded actuator elements. Arrows indicate the slot velocity.

vectors are drawn in the slot. The dashed line indicates the function of (7) and the red line indicates the function $v_x(x)$ given by (8).

Please note that the spatial amplitude distribution is adapted to a TS wave of a certain frequency. In the expected case that two or more waves are to be damped the

actuation of the actuators can be superimposed using a particular spatial amplitude distribution for each frequency. Therefore, also wave packets can be damped using the framework of this paper.

3 Discussion of Different Design Parameters

For the design of the actuator cascade a few parameters can be chosen. The ratio Ξ of the slot width to the element width in streamwise direction can be chosen with only few constraints. Please note that in the application a large value of Ξ can affect the baseflow profile due to the lack of the no-slip boundary condition at the wall. Also, the number of elements in the cascade can be more or less arbitrarily chosen keeping the design of the single actuator element. By miniaturization actuator elements with smaller lengths could be used. Also a change in the baseflow to slower free-stream velocities can reduce the element length compared to the wavelength of the relevant TS waves.

3.1 Slot Width Ratio Ξ

In Fig. 3 the velocity profile v_x of an actuator cascade with seven elements is shown for different values of Ξ . Hereby, the amplitude of each actuator element

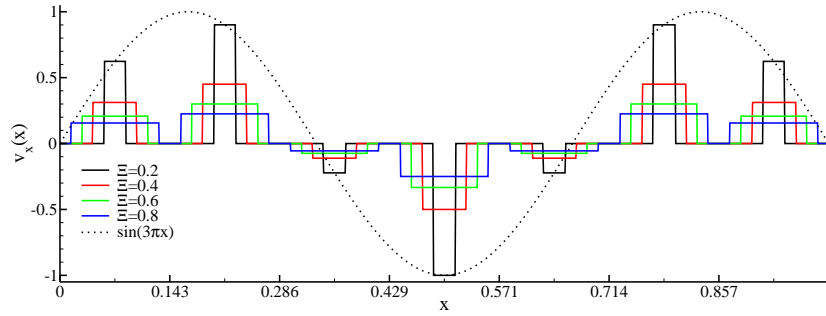


Figure 3 Comparison of spatial velocity distributions with the same blowing ratio Q for different slot ratios Ξ when a TS wave of the wavenumber $\alpha_{TS}L_e = \frac{3\pi}{7}$ is to be generated. A dashed sine function is shown for comparison. The dotted line indicates the function of (7).

is chosen for a TS wavelength of $\alpha_{TS} = \frac{3\pi}{7L_e}$ using (7). The continuous function $v_x(x) = \sin(\alpha_{TS}x + \theta)$ (dotted line)—viable in a numerical simulation—is shown for comparison. The Fourier transforms according to Fig. 3 scaled with the volume flux $\frac{|V_x(\alpha)|}{Q}$ are shown in Fig. 4. All functions have a maximum in the immediate vicinity of α_{TS} and show only slight differences up to a wavenumber of $3\alpha_{TS}$. For higher wavenumbers there are large differences. The higher the slot ratio Ξ , the lower the receptivity for higher harmonics.

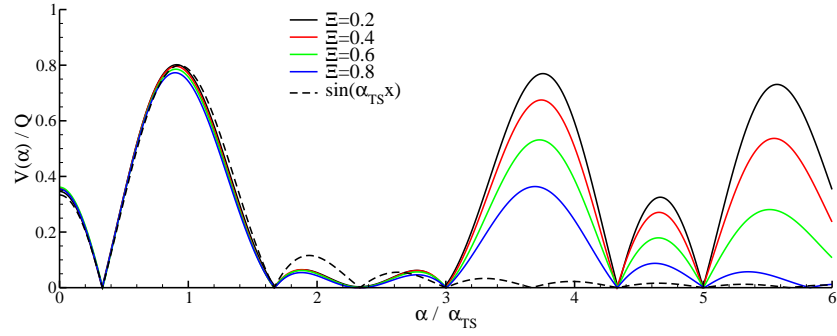


Figure 4 Comparison of the scaled Fourier transform of the blowing and suction profile for different slot ratios Ξ when a TS wave of the wavenumber $\alpha_{TS} = \frac{3\pi}{7L_e}$ is to be generated. A sine function (dashed line) is shown for comparison.

3.2 Phase Parameter θ

Even though the phase parameter θ is not fixed by the geometry it is a parameter which is to be chosen. Varying the phase parameter θ in (7), for $\alpha_{TS} = \frac{2\pi}{7L_e}$ we obtain the functions $\frac{|V_x(\alpha)|}{Q}$ plotted in Fig. 5. The higher the parameter θ , the higher the wavenumber of the first maximum. All curves exhibit secondary maxima which are, in the plotted region, least distinctive for $\theta = 0$. Therefore, a parameter of $\theta = 0$ is preferable here. However, results for other wavenumbers do not show a clear trend. Therefore, the phase parameter has to be adapted to the specific case depending on the wave to be generated.

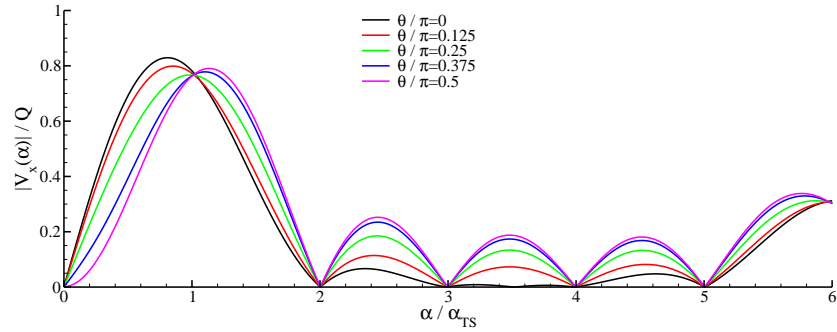


Figure 5 Comparison of the scaled Fourier transform of the blowing and suction profile for different phase parameters θ when a TS wave of the wavenumber $\alpha_{TS} = \frac{2\pi}{7L_e}$ is to be generated using seven actuators. The slot ratio is $\Xi = 0.8$.

3.3 Number of Actuators

For TS waves which have a wavelength of only a few actuator element lengths, e.g. for $\alpha_{\text{TS}} = \frac{\pi}{L_e}$, only a few actuators need to be used to achieve a maximum for $V_x(\alpha_{\text{TS}})$. In Fig. 6 the obtained functions $\frac{|V_x(\alpha)|}{Q}$ are plotted for $\alpha_{\text{TS}} = \frac{\pi}{L_e}$ and $\Xi = 0.5$ when different numbers of actuator elements are used. All curves exhibit a maximum for $\alpha \approx \alpha_{\text{TS}}$. The more elements are used, the narrower are the peaks. However, the size of the peaks cannot be reduced by increasing the number of actuator elements and keeping the same number of elements per wavelength. Comparing the results in Fig. 4 and Fig. 6, we can see that the size of the peaks is smaller in the case with more elements per wavelength. This is due to a better reproduction of a sinusoidal profile. Using more elements gives better results in any case.

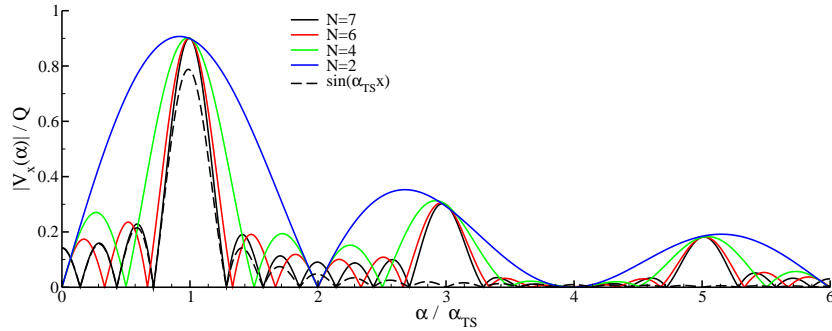


Figure 6 Comparison of the scaled Fourier transform of the blowing and suction profile for a different number of used actuator elements when a TS wave of the wavenumber $\alpha_{\text{TS}} = \frac{\pi}{L_e}$ is to be generated. The slot ratio is $\Xi = 0.5$. The Fourier transform of a sine function (dashed line) is shown for comparison.

3.4 Length per Actuator Element

In Fig. 7, a comparison of the scaled Fourier transform is shown for different numbers of actuators. The overall length of the actuator cascade is kept at the length of the wave to be generated, i.e. $\alpha_{\text{TS}} L_e = \frac{2\pi}{N}$. All functions have a maximum at approximately $\alpha = \alpha_{\text{TS}}$. The higher the number of actuators, the higher is the wavenumber of the first secondary maximum. Furthermore, the functions tend to the function of the continuous sine function.

4 Conclusions

It is shown that setting the velocity amplitude of an actuator element j as $v_{x,j} = \sin(\alpha_{\text{TS}} x_j + \theta)$ with x_j as the streamwise coordinate of the slot center gives good

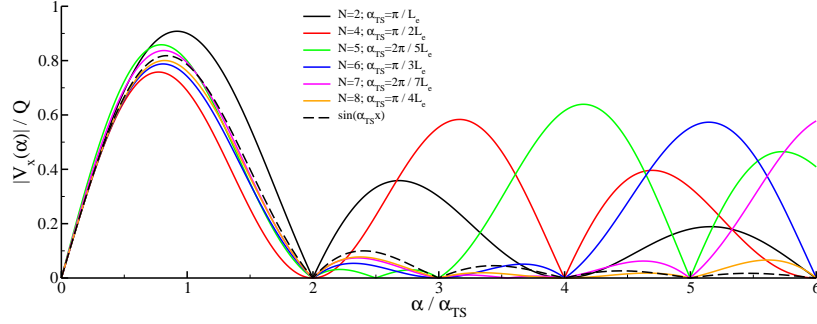


Figure 7 Comparison of the scaled Fourier transform of the blowing and suction profile for a different number of actuator elements. The TS wavelength is fixed to the length of the actuator cascade. The slot ratio and phase parameter is $\Xi = 0.5$ and $\theta = 0$, respectively. The Fourier transform of a sine function (dashed line) is shown for comparison.

results in order to generate or dampen TS waves with the wavenumber α_{TS} . Hereby, the parameter θ needs to be optimized for each particular TS wavelength α_{TS} . In order to keep the receptivity of the higher harmonics of the wave to be generated low, it is pointed out that the Fourier transform of the spatial amplitude distribution $V_x(\alpha)$ is to be minimized for the wavenumbers of the higher harmonics. This can be done by the following measures. First, the number of actuator elements per wavelength is recommended to be set to seven or more elements to reduce the receptivity of the first four higher harmonics and might be increased to reduce the receptivity of further higher harmonics. Secondly, a high ratio of the streamwise slot width to the element width can be used to reduce the receptivity of higher harmonics. Thirdly, increasing the number of actuator elements while keeping the actuator length fixed results in narrower peaks in the Fourier transform, and therefore also reduces the receptivity for higher harmonics.

Acknowledgements

The authors gratefully acknowledge the financial support of the Deutsche Forschungsgemeinschaft (DFG) for the project RI680/18.

References

- [1] C. Gmelin. “Numerische Untersuchungen zur aktiven Dämpfung von Störungen im Vorfeld der laminar-turbulenten Transition.” Dissertation. 2003. Universität Stuttgart.
- [2] E. Laurien and L. Kleiser. “Numerical simulation of boundary-layer transition and transition control” *J. Fluid Mech.* 1989. **199**:403–440.
- [3] M. Marx. “Numerische Untersuchungen und Nichtlineare Optimierung zur Aufstellung einer Berechnungsfunktion für die Rezeptivität der Blasius-Grenzschicht.” Studienarbeit (student research project advised by the authors). 2008. Universität Stuttgart.